

## **Precipitation $^{17}\text{O}$ -excess Altered During Tropical Convection: Evidence from Monsoon Cold Surges in Singapore**

**Yilin Zhang<sup>1,2\*</sup>, Shaoneng He<sup>2</sup>, Bernie Wee Wei Ken<sup>1,2</sup>, Allegra N. LeGrande<sup>3</sup>,  
Jingyu Wang<sup>4</sup>, Nathalie Goodkin<sup>5</sup>, and Xianfeng Wang<sup>1,2</sup>**

<sup>1</sup> Asian School of the Environment, Nanyang Technological University, Singapore 639798, Singapore.

<sup>2</sup> Earth Observatory of Singapore, Nanyang Technological University, Singapore 639798, Singapore.

<sup>3</sup> NASA Goddard Institute for Space Studies, New York, NY 10025, USA.

<sup>4</sup> National Institute of Education, Nanyang Technological University, Singapore 637616, Singapore.

<sup>5</sup> Department of Earth and Planetary Sciences, American Museum of Natural History, New York, NY 10024, USA.

\*Corresponding author: Yilin Zhang ([yilin003@e.ntu.edu.sg](mailto:yilin003@e.ntu.edu.sg))

### **Contents of this file**

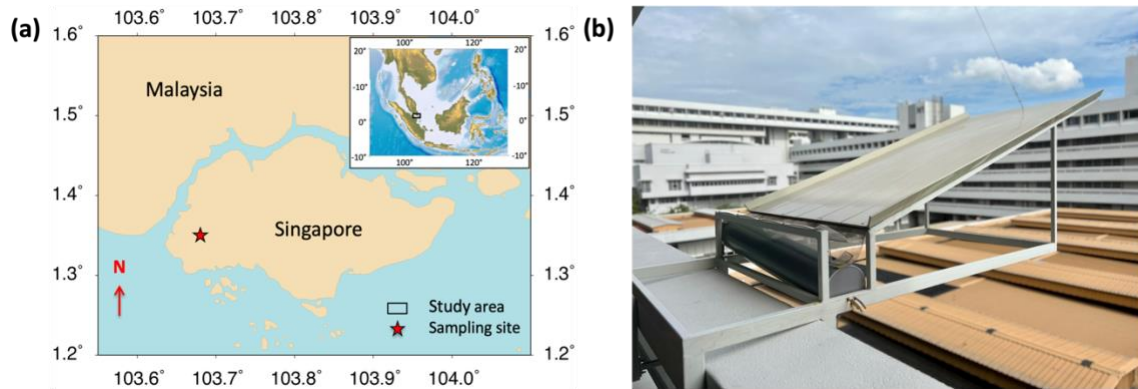
Figures S1 to S8

Table S1

References for the Supporting Information

### **Additional Supporting Information (Files uploaded separately)**

Caption for Data Set S1



**Figure S1.** (a) Regional map with the sampling site at NTU, Singapore (He et al., 2021). (b) Rain collection panel outside the Asian School of the Environment building at NTU designed for continuous and high-temporal resolution sample collection.

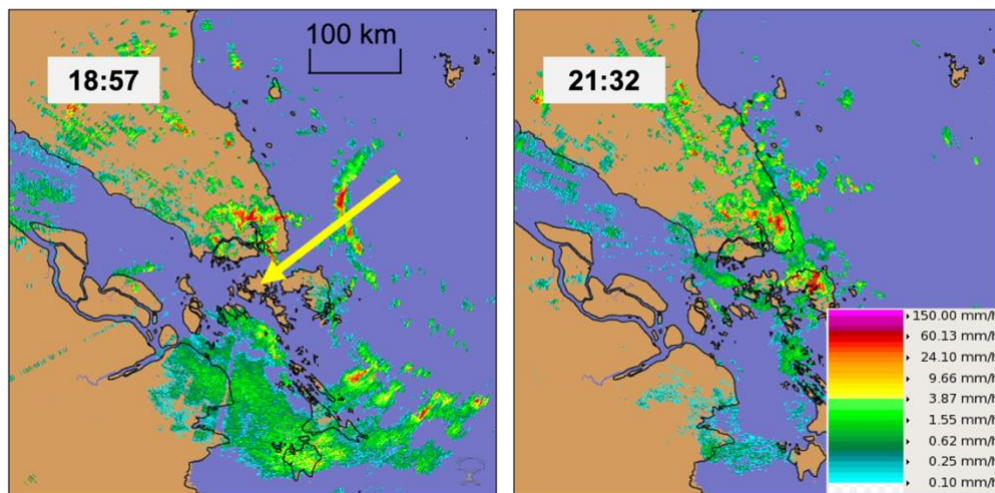


**Figure S2.** Precipitation maps of Northeast monsoon cold surge event over the sampling site on 23<sup>rd</sup> Jan. 2017. The maps are retrieved using the C-band radar reflectivity observations at 5-minute intervals within the radar range of 240 km. Yellow arrow indicates the propagation direction of the monsoon cold surge. Convective zone (e.g., 18:57 at sampling site) is the region with a strong horizontal color gradient, and stratiform zone is generally homogeneous in color.

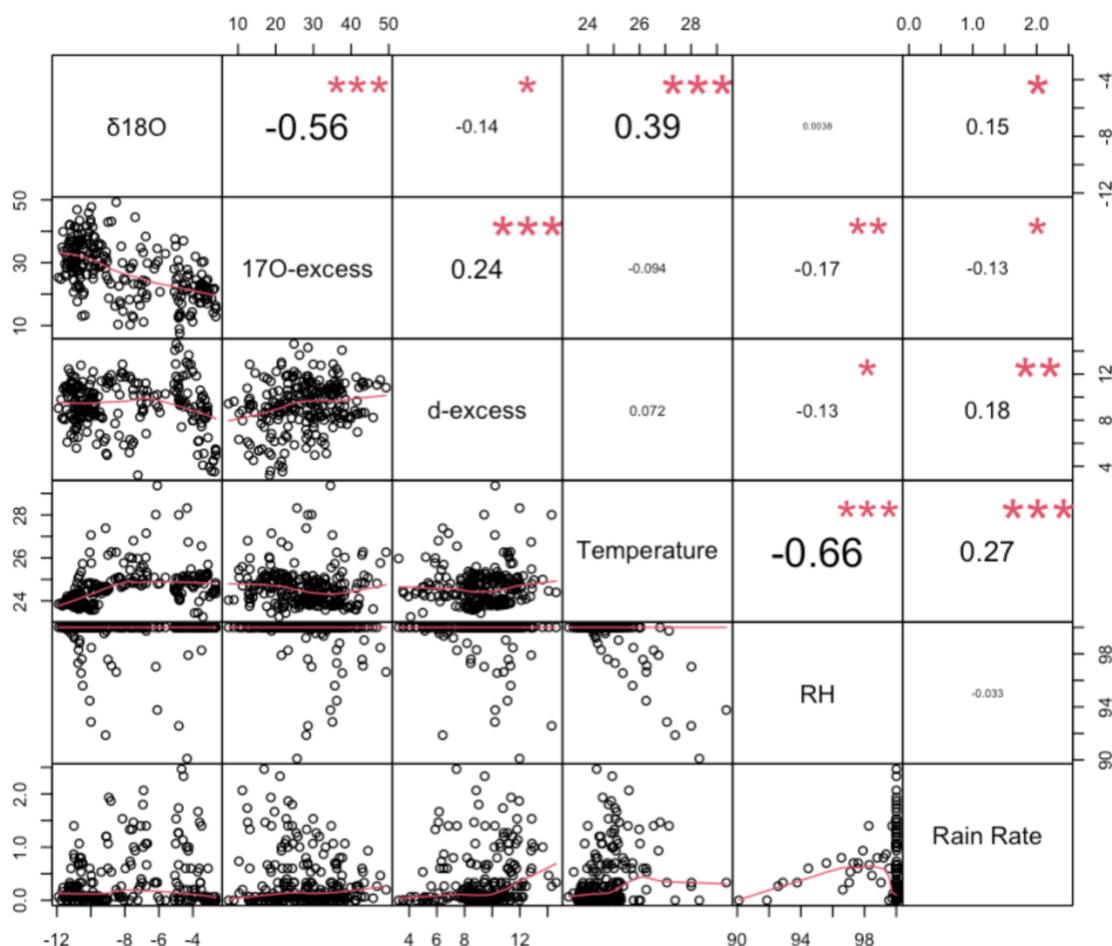


**Figure S3.** Correlation matrix amongst precipitation stable isotope parameters ( $\delta^{18}\text{O}$ , d-excess,  $^{17}\text{O}$ -excess) and on-site climate variables (temperature, RH, and rain rate) for all six rain events combined ( $n=237$ ). The correlation matrix is plotted together with density functions, smoothed regression lines and correlation coefficients (r-value) with the corresponding significance levels in red stars (if no stars, the variable is not statistically significant, while one, two and three stars mean that the corresponding variable is significant at 10%, 5% and 1% levels, respectively).

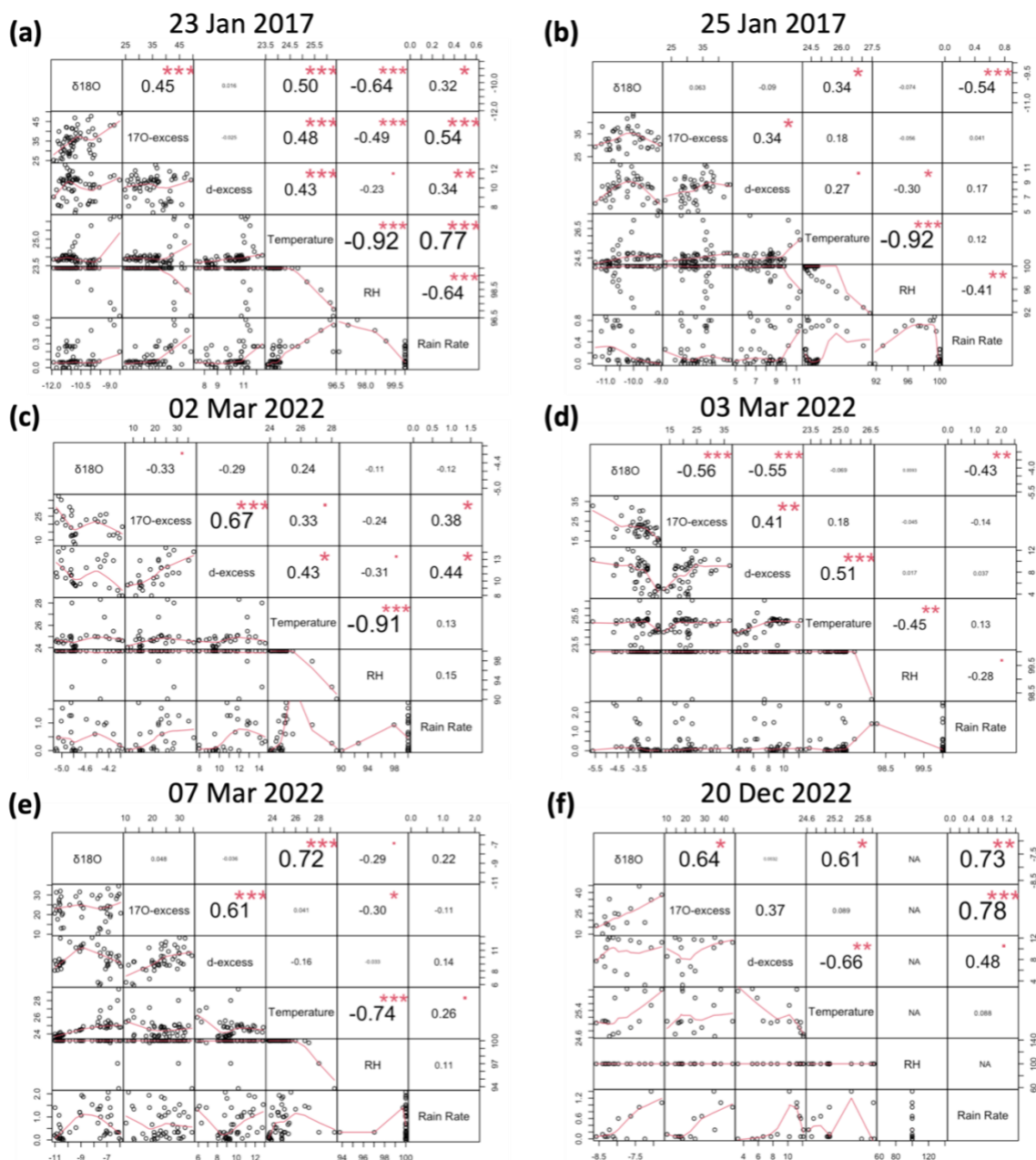


**Figure S4.** Correlation matrix amongst precipitation stable isotope parameters ( $\delta^{18}\text{O}$ , d-excess,  $^{17}\text{O}$ -excess) and on-site climate variables (temperature, RH, and rain rate) for each rain event: (a) 23<sup>rd</sup> Jan. 2017, n=60; (b) 25<sup>th</sup> Jan. 2017, n=44; (c) 2<sup>nd</sup> Mar. 2022, n=30; (d) 3<sup>rd</sup> Mar. 2022, n=42; (e) 7<sup>th</sup> Mar. 2022, n=46 and (f) 20<sup>th</sup> Dec. 2022, n=15. The correlation matrix is plotted together with density functions, smoothed regression lines and correlation coefficients (r-value) with the corresponding significance levels in red stars (if no stars, the variable is not statistically significant, while one, two and three stars mean that the corresponding variable is significant at 10%, 5% and 1% levels, respectively).

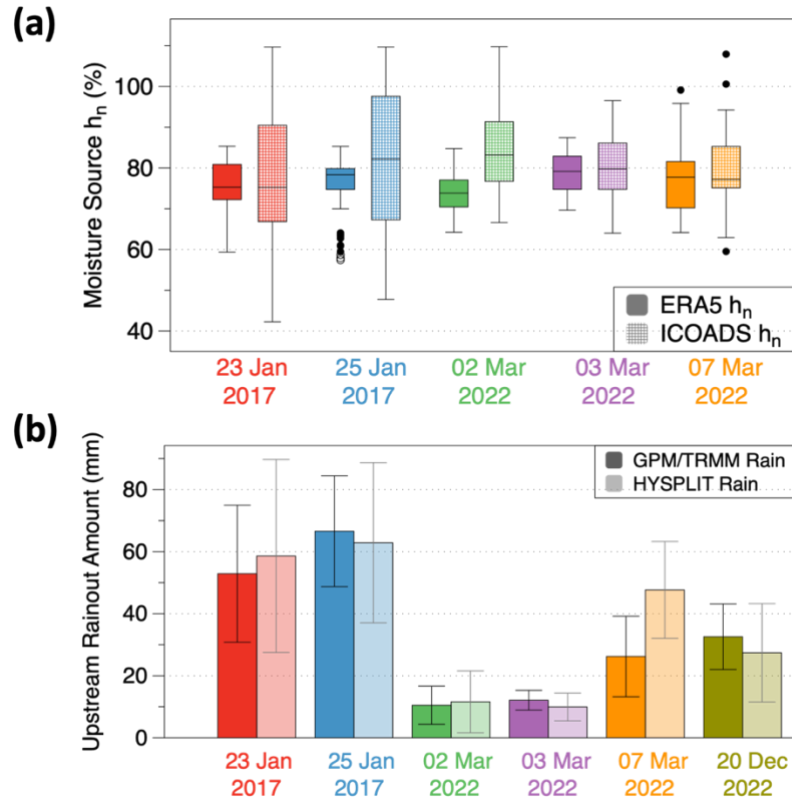


**Figure S5. (a)** Comparison between the moisture source  $h_n$  calculated from both the ICOADS observational data (pattern fill) and ERA5 reanalysis data (solid color fill) based on the same locations. Box represents first and third quartile range and the middle black line indicates median. The maximum and minimum values are indicated by whiskers. The ICOADS observational data was not available for the rain event on 20<sup>th</sup> Dec. 2022. The analysis indicates that the two datasets produce similar  $h_n$  values, suggesting that the ERA5 reanalysis data can be used with confidence in subsequent analyses.

**(b)** The rainout amount calculated from both HYSPLIT and TRMM/GPM data was similar to each other, with a slightly larger discrepancy for the event on 7th Mar. 2022. The graph displays the mean and standard deviation of rainout amount for each event, with error bars showing  $\pm 1$  standard deviation. Overall, the close agreement between the two datasets confirms the robustness of the variations in rainout amount.

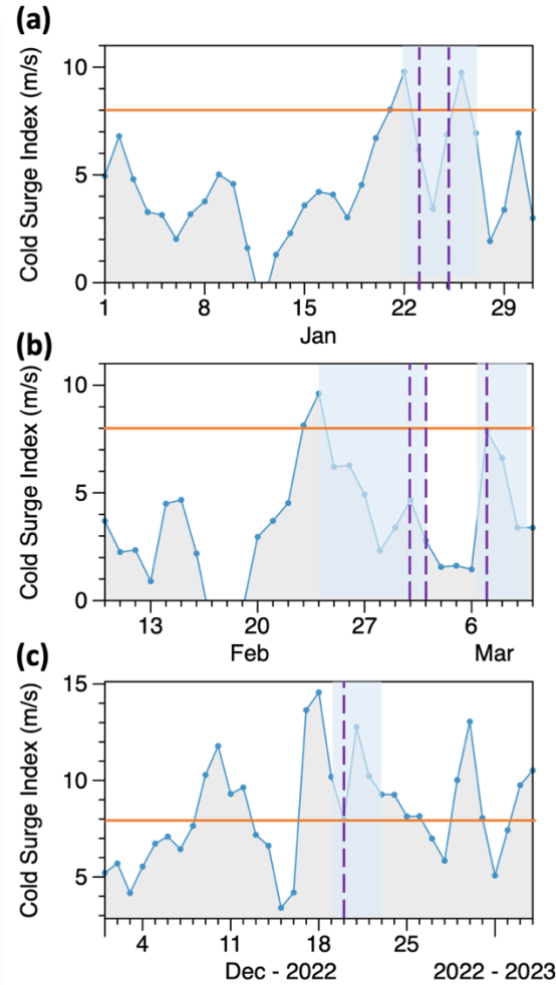


**Figure S6.** Cold surge index upstream from equatorial South China Sea. (a) Jan. 2017; (b) Mar. 2022 and (c) Dec. 2022. The cold surge index was calculated as the average speed of 925 hPa meridional winds between 110°E and 117.5°E at 15°N (Chang et al., 2005). A cold surge index exceeding 8 m/s (orange lines) implies the presence of a strong cold surge system. Purple dashed lines indicate the sampling dates. The blue shadings highlight the span of the cold surge based on daily rainfall in Singapore, as one cold surge event can last between 1 and 5 days. It took around three days for the surge to propagate across the South China Sea from the index calculation location to reach our sampling site.



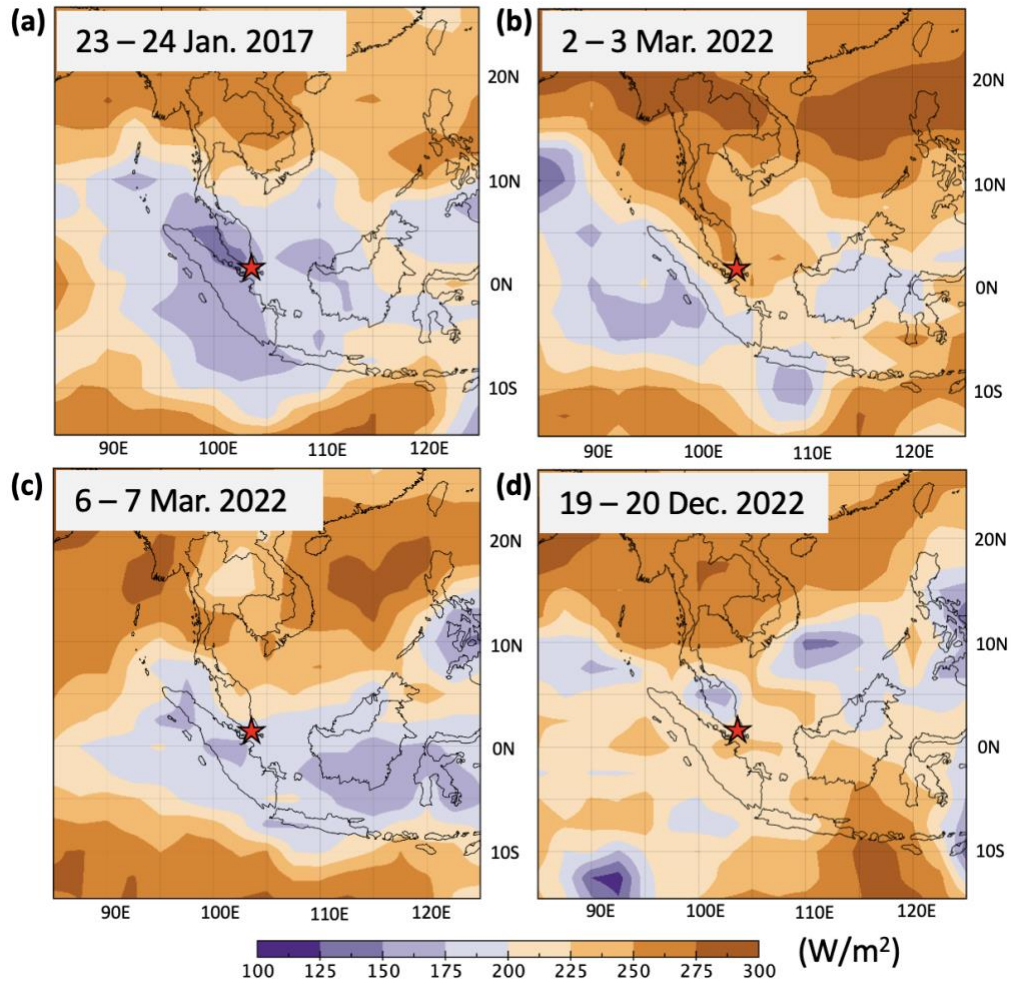


**Figure S7.** Regional map with 2-day interpolated Outgoing Longwave Radiation averaged over: (a) 23<sup>rd</sup> – 24<sup>th</sup> Jan. 2017; (b) 2<sup>nd</sup> – 3<sup>rd</sup> Mar. 2022; (c) 6<sup>th</sup> -7<sup>th</sup> Mar. 2022; and (d) 19<sup>th</sup> – 20<sup>th</sup> Dec. 2022. The area with lower OLR (purple shading) signifies stronger convection. Red star indicates the sampling site. Regional convection in the South China Sea and nearby sampling site is stronger in Jan. 2017 and Dec. 2022 than in Mar. 2022

**Table S1.** Slopes of meteoric water lines (MWLs) defined by precipitation  $\delta^{18}\text{O}$  and  $\delta^2\text{H}$  for the convective zone, stratiform zone and the entire event across all six rain events.

<b>Rain Event</b>	<b>23 Jan 2017</b>	<b>25 Jan 2017</b>	<b>02 Mar 2022</b>	<b>03 Mar 2022</b>	<b>07 Mar 2022</b>	<b>20 Dec 2022</b>
<b>Convective Zone</b>	7.77	9.18	8.41	7.24	7.53	6.88
<b>Stratiform Zone</b>	7.53	5.74	6.23	5.46	9.48	4.18
<b>Entire Event</b>	8.03	7.79	6.44	5.94	7.96	8.01

**Note.** The slope of MWL in the stratiform zone for the event on 7<sup>th</sup> Mar. 2022 (9.48) may be subject to bias due to a limited number of data (n=7).



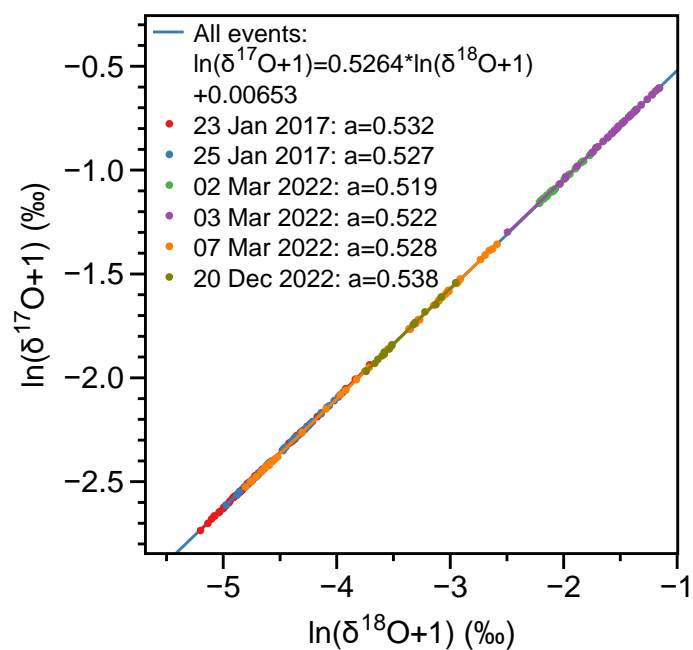


**Figure S8.**  $\ln(\delta^{18}\text{O} + 1)$  versus  $\ln(\delta^{17}\text{O} + 1)$  for all events combined and each individual event. 'a' represents the slope of the meteoric water lines for each event.

**Data Set S1.** Sample ID, collection time, precipitation  $\delta^{18}\text{O}$ ,  $\delta^2\text{H}$ ,  $\delta^{17}\text{O}$ , d-excess,  $^{17}\text{O}$ -excess, onsite temperature, relative humidity and rain rate for the six rain events investigated in this study.